ELSEVIER

Cryogenics 39 (1999) 53–58

Cryogenics

Superconducting magnetic energy storage device operating at liquid nitrogen temperatures

A. Friedman *, N. Shaked, E. Perel, M. Sinvani, Y. Wolfus, Y. Yeshurun

Institute for Superconductivity, Department of Physics, Bar-Ilan University, Ramat-Gan 52900, Israel

Received 7 July 1998; received in revised form 7 November 1998

Abstract

A laboratory-scale superconducting energy storage (SMES) device based on a high-temperature superconducting coil was developed. This SMES has three major distinctive features: (a) it operates between 64 and 77K, using liquid nitrogen (LN_2) for cooling; (b) it uses a ferromagnetic core with a variable gap to increase the stored energy while retaining the critical current value; (c) it has the option for simultaneous energy charge and discharge which increases the power available at the SMES output by a factor of ≤ 2 when operating as a converter. The present prototype of liquid nitrogen operating SMES stores 130 J at 64K and 60 J at 77K.

Keywords: High T_c superconductors; Critical current density; SMES; Power applications

1. Introduction

A device for storing electromagnetic energy is an attractive potential application for high-temperature superconductors (HTS). The feasibility of a high-temperature superconducting magnetic energy storage (HT-SMES) device has been extensively discussed [1–4] and a few experimental projects aiming at operating temperatures of ~ 30K were reported [5–8].

The two main obstacles delaying the development of a LN_2 operated SMES are the relatively low critical current density J_c of the BSCCO wires and the strong decrease of J_c with magnetic field at LN_2 temperature. These two factors result in low values for the stored energy, making the liquid nitrogen operated SMES inefficient i.e. with poor ratio of the maximal energy stored in the coil to the power required for its cooling. Calculations [9] show that for BSCCO-based SMES, maximum efficiency is achieved at about 30K. We report here on an HT-SMES, based on HTS coil made of Bi–Sr–Ca–Cu–O (Bi-2223) wires, operating at liquid nitrogen (LN_2) temperatures. In order to improve the efficiency of this SMES we have introduced a ferromagnetic core and designed a special converter circuit. The core, made of laminated iron surrounding the HTS coil, contributes a gain of $\times$ 14 and $\times$ 6 in the stored energy at 77 and 64K, respectively. Moreover, the core is designed to prevent the coil from being exposed to the magnetic self-fields, allowing for relatively high operation currents in the presence of high self-fields. A specially designed converter enables simultaneous charge and discharge of the HTS coil, adding another factor of $\leq$ 2 in the transmitted power. The details of this SMES and its operational states are described below.

2. SMES structure

2.1. The HTS coil

The three double pancakes coil, purchased from American Superconductors Corporation (ASC) is made of 160 m multifilamentary silver-sheathed BSCCO wire. Its critical current (1 μV/cm criterion) is 22.2 A at 77K. The energy storage capacity at this temperature is 4.2 J. Table 1 summarizes the characteristics of this coil.

Typical I–V curves for the coil are shown in Fig. 1 for 64 and 77K. All measured I–V curves between 52 and 77K exhibit a power law dependence: $V = V_0(I/I_c)^n$, with a power n between 10 and 12. The critical current, I_c, was found to increase, approximately lin-

* Corresponding author.

0011-2275/99/$ - see front matter
PII: S0011-2275(98)00126-X

Table 1
Characteristics of the HTS coil

Inside diameter (mm)	194
Outside diameter (mm)	244
Height (mm)	18
Number of turns	250
Conductor length (m)	160
Inductance (mH)	17
Critical current @ 77K (A)	22.2
Maximal amperturns @ 77K	5550
Stored energy @ 77K (J)	4.2

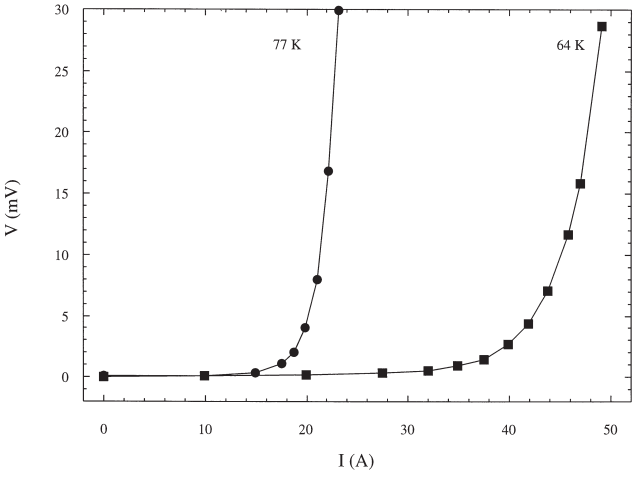

Fig. 1. I–V curves of the HTS coil at the indicated temperatures.

early, with decreasing temperature, in agreement with previous reports for HTS coils [10].

We also investigated the interplay between AC and DC currents and their influence on the measured I–V curves. We observed that the application of a sinusoidal current component in the frequency range of 50–500 Hz, in the presence of a DC level in the range of 16–22.5 A, caused a significant increase in the DC voltage. The DC voltage increment due to the AC component was found to increase linearly with the frequency and with the DC current level, and quadratically with the AC amplitude. This phenomenon is discussed elsewhere [11].

2.2. Ferromagnetic core

The possible gain in field and energy by inserting a magnetic core into the coil was analyzed by Cha using a long solenoid approximation and finite element calculation [12]. The use of a ferromagnetic core inside the coil was shown to increase the stored energy only at low current densities. Morisue et al. [13] examined the gain in the stored energy for a ferromagnetic cylinder placed outside the coil with internal fields up to 4 T. While this gain was shown to be significant, their configuration induces an increase in the field experienced by the coil and thus a decrease in its critical current.

In the present work we have investigated the gain in the stored energy for a 'closed core' configuration. In this configuration, the core occupies the volume both inside and outside the coil. This prevents flux lines from leaking out of the core increasing the field at the coil site. Energy gain calculations for several geometrical shapes of closed cores are given elsewhere [14]. To illustrate the conclusions from these calculations we focus here on a special case of a closed core namely, the 'pot core' configuration in which the cross section S_0 along the flux path is kept constant, so that the 'leakage' of flux out of the core is negligible.

The maximal energy stored in a coil surrounded by a nearly saturated pot core can be estimated [14] as

$$U = \frac{1}{2} LI^2 \approx \frac{1}{2} B_s INS_0 \quad (1)$$

where L is the inductance of the coil with the core, I is the current flowing in the coil, N is the number of turns and B_s is the saturation magnetic induction in the core.

According to Eq. (1), the energy gain due to the iron core is proportional to the increase of the inductance or, equivalently, to the induction gain.

The term $LI^2/2$ in Eq. (1) indicates the importance of the interplay between the current I and the inductance L. With a ferromagnetic core the current increase may drive the core into saturation where the inductance drops dramatically. It is therefore crucial to select an operation current close to the critical current which drives the core as close as possible to the saturation point, but still in the high inductance regime. To achieve the optimal working conditions we have introduced a variable gap into the core. As the gap width increases, the coil inductance below the saturation decreases. This allows for larger currents in the coil resulting in a total increase in the stored energy. By varying the gap we are able to operate the same construction at different temperatures i.e. different values of the critical current. For technical reasons, in the present work the core occupies only 40% of the optimal volume of a pot-core configuration. The expected energy gain for 100% of the available volume is thus larger by a factor of ≈ 2. The characteristics of the core used in our device are summarized in Table 2.

The data presented in Table 2 might suggest that the energy gain decreases with increasing stored energy. It is important to note that the energy gain obtained by the core insertion strongly depends on the magnetic field of the coil without a core. To obtain a significant gain at low temperatures where the critical current and the stored energy are high it is necessary to design the coil to have a low self induction. This conclusion will also hold for future HTS wires which will probably offer much higher critical currents at high temperatures.

The core was made of thin sheets of commercial silicon steel formed into a standard C-core shape. Pairs of

Table 2
Parameters of the core

	52K	64K	77K
Air gap (mm)	13.3	9	4.1
Core cross-section (m^2)	0.013	0.013	0.013
Critical current (A)	72	49	22.2
Energy without core (J)	44	20.4	4.2
Energy with core (J)	193	131	59.4
Energy gain E/E_0	4.4	6.4	14.1
Expected gain for 100% volume	9.3	13.6	30
Inductance without core (H)	0.017	0.017	0.017
Inductance with core (H)	0.075	0.11	0.24
Maximum field with core (T)	1.7	1.7	1.7
Maximum field without core (T)	0.39	0.27	0.12

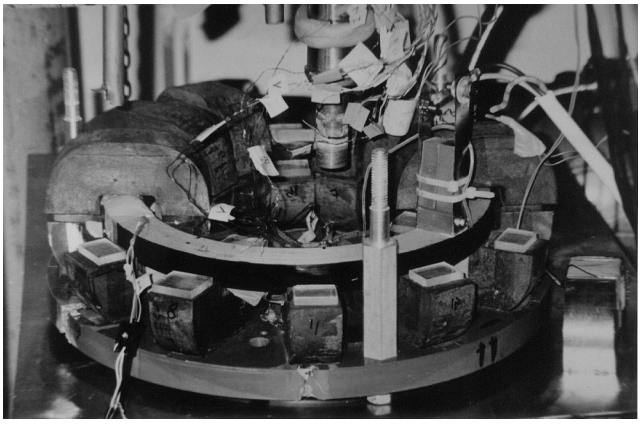

Fig. 2. The coil with the core (for clarity some of the C-cores are removed).

these C-cores form rings surrounding the coil. PVC spacers were inserted between the C-cores to form the appropriate gap at the desired operating temperature. Fig. 2 shows a photograph of the coil and the core. For clarity we removed several of the C-core elements.

2.3. Electric circuit

The electric circuit of our SMES device is sketched in Fig. 3. An important part of the circuit is the converter

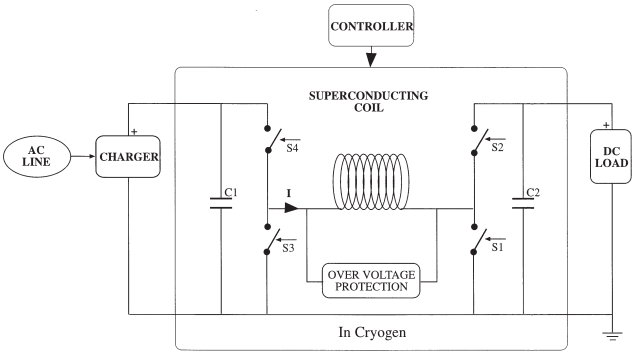

Fig. 3. Electric circuit of the SMES.

which generates positive and negative voltage pulses to charge and discharge the superconducting coil. Two capacitor arrays, at the charger (C1) and at the load (C2), are used for the conversion of voltage to current in the coil, and vice versa. The coil is connected to four switches (Fig. 3), forming an open bridge configuration, and protected against overvoltage that might occur during a fault. The switches are responsible for the different basic states of operation. When switches 1 and 4 are closed and 2 and 3 are open, the superconducting coil is **charged** from the DC power source. When switches 2 and 3 are closed and 1 and 4 are open, the **discharge** state is obtained. In this state a current is withdrawn from the coil and fed into the load capacitor to create the load voltage. When switches 1 and 3 are closed and 2 and 4 are open the coil is in the '**persistent**' state and the current flows in a closed loop within the superconducting coil. The persistent state is set as an intermediate state when charge or discharge states are not required. The switches settings for the different states are summarized in Table 3.

To reduce energy losses in the converter, most of its elements were immersed in liquid nitrogen. The resistance of the switches drops from 7 mΩ at room temperature to 2 mΩ at LN_2 temperatures. As shown in Table 3 and Fig. 3, switch 2 plays the role of a diode. We have found that MOSFET transistors exhibit low resistance in comparison with other kinds of electronic switches and diodes at LN_2 temperatures. Two kinds of capacitors were used as charger and load capacitors. One capacitors bank, which carries high currents, was immersed in the

Table 3
Switches settings for the various operation states of the SMES

State	S1	S2	S3	S4
Charge	Closed	Open	Open	Closed
Persistent	Closed	Open	Closed	Open
Discharge	Open	Closed	Closed	Open
Through	Open	Closed	Open	Closed

LN_2 to reduce the losses in the wires. For this bank we have used polyester capacitors that have low energy density but they maintain their capacitance at 77K. The remaining part—tantalum capacitors—were placed in the upper part of the dewar at temperature of about 0°C.

The logic that governs the above switching circuit is described in Fig. 4. The SMES can also operate in a converter mode in which the coil is automatically switched between the three operating states according to the load voltage and the coil current conditions. The field and current probes sense actually the amount of the electromagnetic energy stored in the SMES. The reading of these sensors is compared with two limit values at the comparators. Once the coil current decreases below the lower limit value, the controller sets the switches into the **charge** state. The charge state is maintained until the current achieves its preset upper value. The voltage sensor senses the voltage across the load. This value is again compared with two limiting values. Below the minimal value, the **discharge** state is set until the load voltage reaches its maximum value. The limiting values of the coil current and the load voltage can be set by the user. Between these two states, when no charge or discharge is required, the current circulates in the coil. In this **persistent** state the loss of energy depends on the coil current and on the resistance of switches 1 and 3. At the critical current at 77K this loss is about 1 W. To compensate for the energy loss the coil is charged with 1 ms pulses of 10 V at a frequency of 5 Hz.

A unique feature of our SMES device operating as a converter is the ability for a simultaneous charge/discharge operation [15]. In this improved mode, charging the HTS coil can overlap its discharging. The benefit of this configuration is clear: the independent operation of the charge/discharge states enables the duration of each state to be stretched up to a full cycle. For the common case, when the charger voltage is equal to the output DC voltage, this doubles the available power at the device output, while the coil dimensions and operation costs remain unchanged. The simultaneous charge/discharge state is achieved when switches 2 and 4 are closed and switches 1 and 3 are open. This state appears in Table 3 as a 'through' state. It is important to note that in this state charging and discharging are still independent.

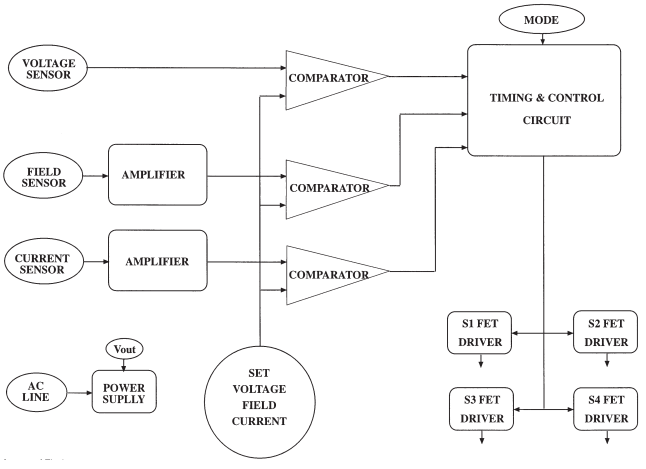

Fig. 4. Control circuit of the converter.

2.4. Cryogenics

The benefits of LN_2 operation arise from the increase of cooling efficiency with the increase of the operation temperature and from the excellent thermal contact between the coolant and the HTS coil. On the other hand, the critical current drops dramatically with the increase of temperature and field, resulting in a decrease in the amount of stored energy. It is, thus, necessary to balance between these two conflicting effects in order to find the optimum operation temperature. Following Stephanblome, Kellers and Kleimaier (SKK) [9], we define a 'figure of merit' for the SMES as the ratio of stored energy and the power required to cool the system. The stored energy is given by

$$0.5LI_c^2$$

and the cooling power is taken to be proportional to that of an ideal Carnot machine i.e. $T/(T_{RT} - T)$, where T is the operating temperature and T_{RT} is the room temperature. From the measured $I_c(T)$, and from the known temperature dependence of the cooling power of the Carnot refrigerator, SKK calculated the figure of merit for an HTS coil as a function of temperature. This figure of merit exhibits a maximum around 30K (circles in Fig. 5). SMES operation is practical between the 3 db point i.e. 8–62K. This situation is significantly changed with the introduction of iron core where the dependence of

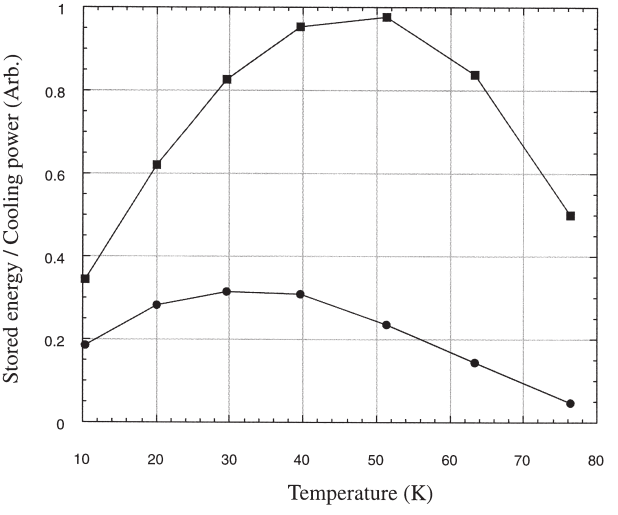

Fig. 5. Figure of merit for the HTS coil with (■) and without (●) magnetic core, as a function of temperature.

the stored energy on the operation current becomes weaker (see Table 2). As a result, the calculated figure of merit (squares in Fig. 5) exhibits a maximum around 50K, upwarding the practical range (between the 3 db points) to 15–77K, overlapping with the regime of LN_2 temperatures.

The HTS coil, the core and part of the electric circuit (marked in a rectangular frame in Fig. 3) are immersed in LN_2. While operating, the heat generated by the SMES causes additional losses of 0.1 l/h, which is about 30% of the overall cooling losses in our dewar.

The main sources for the operation losses are the ohmic components in the device. We have therefore selected electric components that are suitable for operation at LN_2 temperatures. The losses due to these components are much lower at low temperatures than at room temperature.

The working temperature was achieved by controlling the vapor pressure of the LN_2. The SMES operation was tested between 52K (solid nitrogen) and 77K. Although pumping adds to the cost of operation, it adds flexibility in choosing the working temperature, allowing for an increase in the stored energy and power.

To avoid working in solid nitrogen which offers inferior thermal contact than the liquid, we have selected the operation temperature to be ~ 64K, which is slightly above the triple point of nitrogen ($T - 63.2$K). This temperature is achieved at a vapor pressure of about 100 Torr that is accessible by a low power-consuming rotary vacuum pump. The liquid state of nitrogen ensures ideal cooling conditions of the coil and other elements of the electric circuit.

3. Operation

Integration of the components described above results in a SMES device operating in the temperature range between 64 and 77K with a stored energy of up to 130 J (at 64K). This device supplies a stable DC voltage to the load, which does not depend on the power quality of the input AC line.

For a persistent current of 15 A the losses per second at 77K are, on the average, ~ 0.5% of the stored energy. These losses are mainly a result of the ohmic components of the circuit. At this current, the intrinsic losses of the superconducting coil are two orders of magnitude less than the ohmic losses and are negligible.

Fig. 6 demonstrates the operation of the SMES at 77K. The first 2 s show its operation as a converter, with a load of 6 W. In this mode, energy of 50 J is stored in the coil while pulses of negative and positive voltage, shown in the lower left part of the figure, charge and discharge the coil. The need for a charge or discharge pulse is determined by the control circuit which probes the coil current and the load voltage. Simultaneous

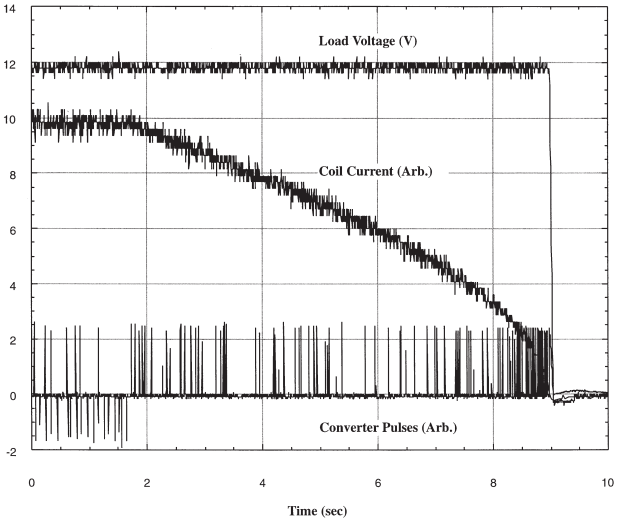

Fig. 6. Operation of the SMES device at 77K as a function of time. The upper curve is a record of the load voltage. Charge (negative) and discharge (positive) pulses are shown in the lower part of the figure. The middle curve records the coil current which is proportional to the square root of the stored energy.

appearance of charge and discharge pulses are apparent in the figure. After approximately 2 s the SMES was disconnected from the AC line in order to simulate a power failure. Fig. 6 shows that while the charge pulses are stopped, the discharge pulses continue so that the voltage across the load (the upper curve in the figure) is kept constant. As the energy stored in the coil decreases (middle curve), the frequency of the discharge pulses increase because each pulse converts less energy. When the stored energy reaches a predefined lower limit (in our case it is 4% of the stored energy), the SMES operation is stopped and the output voltage drops to zero. It is important to note that throughout all the time of SMES operation the output voltage remains constant. The ripple seen in the voltage curve (upper curve) is a user defined value and may be set to a value as low as required. For a lower ripple value the discharging pulses will become narrower but more frequent. In this case losses in the SMES device grow as a result of the increase in the rate of switching operations.

4. Summary

We have designed, built and tested a prototype of SMES operating in the temperature range between 64 and 77K using liquid nitrogen cooling. This method of cooling offers a good thermal contact between the coolant and the device, it provides good thermal stability and homogeneity, and therefore is suitable for large scale applications.

We have used a ferromagnetic core to increase the stored energy in our SMES. A variable gap was intro-

duced to match the device inductance with the critical currents at different temperatures. Calculations for the present experiment suggest a factor of ~ 30 in the energy gain at 77K for optimal core design.

The insertion of magnetic core should be considered carefully in every SMES device. For low temperatures, the gain in the stored energy may be low and the core may become large and costly. On the other hand, it is clear that for high temperature operation with the present wire technology the energy gain is much higher, hence the cost of the core and its additional weight are worthwhile.

A converter circuit was designed to convert the current stored in the coil to a constant voltage across the load. It allows also the operation of the SMES as a DC–DC converter with simultaneous charging and discharging pulses, yielding an increase of up to a factor 2 in the power that can be supplied by the device. The possibility for simultaneous charge and discharge operation may contribute to any converter device using a superconducting coil [15].

Acknowledgements

We thank Gadi Pinkovich for help in the converter construction. We also thank J. Kellers and A.P. Malozemoff of ASC Inc. for useful discussions and for sharing with us available information. The Ministry of Energy and Infrastructure supported this work under contract no. 93-11-039. A.F. acknowledges a support from the Ministry of Sciences and Humanities under contract no. 6781-1-95.

References

[1] Eyssa YM, Abdelsalam MK, Boom RW, McIntosh GE. Cryogenics 1988;33:69–75.
[2] Schoenung SM, Bieri RL, Meier WR, Bickel TC. IEEE Transactions in Applied Superconductivity 1993;3:200–3.
[3] Schoenung SM, Meier WR, Fagaly RL, Heiberger M, Stephens RB, Stephens J, Leuer JA, Guzman RA. IEEE Transactions in Applied Superconductivity 1993;8:33–9.
[4] Akita S, Wachi Y, Meguro S, Saito T, Kazuhiro U, Kazuhiko N, Takakazu S. In: Design Study of High-T_c SMES. Supporo, 1996.
[5] American Superconductors, Inc., Transforming the grid. Annual Report, 1996.
[6] American Superconductors Inc., Revolutionizing the way the world manages energy. Annual Report, 1997.
[7] Kalsi SS, Aized D, Connor B, Snitchler G, Campbell J, Schwall RE, Kellers J. IEEE Transactions in Applied Superconductivity 1997;7:971–6.
[8] Paasi J, Lahtinen M, Lehtonen J, Mikkonen R, Söderlund L, Connor B, Kalsi SS. Proc. of MT-15 Conference, Beijing, China, October 20–24, 1997:781–4.
[9] Stephanblome T, Kellers J, Kleimaier M. Private communication, 1995.
[10] Ueyama M, Ohkura K, Kobayashi S, Muranaka K, Kaneko T, Hikata T, Hayashi K, Sato K. In: Proceedings of the 7th International Symposium on Superconductivity, (ISS94), Japan, 1995, p. 847.
[11] Shaked N, Al-Omari IA, Friedman A, Wolfus Y, Sinvani M, Shaulov A, Yeshurun Y. Applied Physics Letters 1998;73:3932–4.
[12] Cha YS. Journal of Applied Physics 1993;73:6787.
[13] Morisue T, Yajima T. Journal of Applied Physics 1994;75:6969.
[14] Friedman A, Shaked N, Sinvani M, Wolfus Y, Yeshurun Y. Unpublished, 1998.
[15] Yeshurun Y, Perel E, Friedman A, Shaked N, Sinvani M, Wolfus Y. US patent 60/071852, 1998.